Journal of Organometallic Chemistry 696 (2011) 3376–3383

Contents lists available at ScienceDirect

Journal of Organometallic Chemistry

journal homepage: www.elsevier.com/locate/jorganchem

Intramolecular rearrangement of the imine–amide ligand within the nickel coordination sphere affected by carbon monoxide

Peter B. Kraikivskii [a,b,*], Hans-Friedrich Klein [a], Vitaly V. Saraev [b], Nils E. Schlörer [c], Victoria V. Bocharova [b]

[a] Eduard-Zintl-Institut für Anorganische und Physikalische Chemie der Technischen Universität Darmstadt, Petersenstrasse 18, 64287 Darmstadt, Germany
[b] Department of Chemistry, Irkutsk State University, Str. K. Marks 1, 664003 Irkutsk, Russia
[c] Department für Chemie, Universität zu Köln, Greinstrasse 4, 50939 Köln, Germany

ARTICLE INFO

Article history:
Received 7 June 2011
Received in revised form
13 July 2011
Accepted 18 July 2011

Keywords:
Nickel
Diimine ligands
Chelates
Structure elucidation

ABSTRACT

The interactions of the nickel imine–amide allyl complex $[D^2\text{-}(\overline{C{=}N\hat{}N{-}C})Ni(\eta^3\text{-allyl})]$ **1** with carbon monoxide and unsaturated hydrocarbons have been studied. It is shown that this complex reacts readily with carbon monoxide to form the nickel(0) diimine carbonyl complex [(2-(1-propenyl)-[1,10]phenanthroline)$Ni(CO)_2$] **2**. During the process the ligand undergoes a deep transformation within the nickel coordination sphere. Specifically, the nickel–nitrogen σ-bond turns to an N-donor bond with aromatization of a ring in the nitrogen-containing ligand. This novel heteroaromatic ligand 2-(1-propenyl)-[1,10] phenanthroline has been isolated; the nickel(0) diimine carbonyl complex **2** has been studied with X-ray diffraction method. The comparative spectral studies of complexes **1**, **2**, and 2-(1-propenyl)-[1,10]phenanthroline have been carried out with UV/vis, IR-FT, and 2D NMR spectroscopy. It has been shown that the planar 16-electron nickel(II) imine–amide allyl complex **1** is indifferent to olefins and acetylenes. Based on the NMR data, this fact can be explained by the inability of the π-δ rearrangement into **1**.

1. Introduction

Polymerization of olefins is still one of the most important industrial processes today and α-olefins are the most valuable products. In 1995 the work of Brookhart et al. [1] on the usage of nickel and palladium α–diimine complexes for polymerization attracted attention of the scientific community at large. It served as a powerful stimulus for studying diimine complexes of transition metals in polymerization of both linear and cyclic olefins [2–7]. Transition metal allyl complexes with nitrogen-containing ligands are the most interesting subjects for investigations as they bear an active metal–carbon bond inside their coordination sphere that makes such systems promising for organic fine chemicals synthesis and metal complex catalysis [8–12].

The least known today is the possibility of transformations of N-containing ligands themselves within transition metal coordination sphere. For this reason almost all catalytic cycle schemes proposed in the literature, including activation and deactivation of the active species, ignore the possibility that the nature of metal–ligand bonds and, furthermore, the diimine ligand itself can alter. It can be stated that ligands are usually regarded as an unchanging unit which can be "hosted" in the metal coordination sphere or driven out of it in the course of catalytic cycle. It is generally accepted that the state of a transition metal can alter radically at different steps of the catalytic cycle, whereas the possibility of any transformations of ligands is neglected as a rule [3,13–19]. Nevertheless, every aspect of the ligand behavior should be understood and intelligently used, because it may be the only way to atom-economic catalytic systems most consistent with the principles of green chemistry.

The possibility of a profound transformation of diimine ligands within the coordination sphere of a nickel π-allyl complex was demonstrated in [20]. The process involves formation of a nickel–nitrogen σ-bond and an imine–amide complex. Interestingly, phenanthroline, usually a stable ligand, looses aromaticity in one of its heteroatomic rings under very mild conditions (Scheme 1):

Our work focuses on the chemical properties of complex **1**, specifically, whether there is a possibility for this spontaneously formed imine–amide complex to undergo further transformations inside the nickel coordination sphere when affected by the conventional catalytic ligands such as olefins, acetylenes, and carbon monoxide. We hope that our research will help in following the ways of how nitrogen-containing ligands transform that could complement the catalytic cycle puzzle and facilitate the development of catalytic systems with desired properties.

* Corresponding author. Department of Chemistry, Irkutsk State University, Str. K. Marks 1, 664003 Irkutsk, Russia.
E-mail address: peter10@list.ru (P.B. Kraikivskii).

0022-328X/$ – see front matter © 2011 Elsevier B.V. All rights reserved.
doi:10.1016/j.jorganchem.2011.07.022

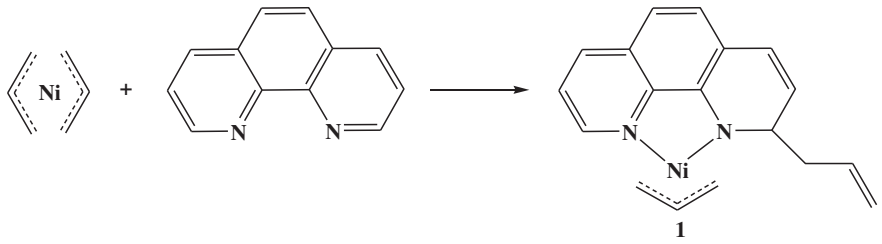

Scheme 1.

2. Results and discussion

Nickel di- and monoallyl complexes are classic catalysts for conversions of olefins, dienes and acetylenes [8]. According to an X-ray structural analysis and multinuclear 2D NMR spectroscopy [20] **1** has a planar structure, contains a π-allyl group, an active fragment, and, besides, it is electron-deficient with its 16-electron pattern. On the whole complex **1** meets all the conventional requirements for a catalyst [21]. This complex is to be active in catalytic conversions of unsaturated hydrocarbons or at least in some interactions with them. We tried to initiate reactions between **1** and ethylene, propylene, norbornadiene, styrene, acetylene, and phenylacetylene. The molar ratios between **1** and the unsaturated hydrocarbons varied from 1:1 to 1:100, while the reaction temperature varied from 20 to 70 °C. Under these conditions the NMR spectra of complex **1** remained unchanged. We could observe only a superposition of chemical shifts from **1** and the used unsaturated hydrocarbon. Of special interest is the fact of a total indifference of **1** toward acetylene and phenylacetylene, as it was quite logical to assume loss of the allyl group by acetylenes due to the acetylene acidic proton. This irritating inertness provoked further tests of **1** with carbon monoxide.

When carbon monoxide was admitted to a bright green ether solution of **1** in a flow reactor, the color quickly changed to bright red followed by a partial fading during 10–14 h. Using GC–MS it was established that the moment of the initial color change was accompanied by formation of acrylic aldehyde in the amount equimolar to the nickel. Further the content of acrylic aldehyde stayed constant in the course of the process.

When the change in the coloration ceased, the crystalline (1:1)-adduct consisting of complex **2** and 2-(1-propenyl)-[1,10]phenanthroline (**pphen**) was obtained from the solution. We studied the molecular structure of the adduct with X-ray structural analysis (the structure is shown on Fig. 1; the crystal packing is given in Supplementary material).

According to NMR data, dissolution of the adduct in THF or toluene does not bring about an interaction between **2** and **pphen**. The ^{1}H NMR spectrum shows a simple superposition of signals from **2** and **pphen** (Fig. 2). The solution contained **2** and **pphen** in approximately equimolar amounts as follows from the corresponding integral intensities of the ^{1}H NMR signals. Analysis of the TOCSY and NOESY spectrum reveals no mutual cross-peaks for **2** and **pphen**.

Analysis of the summation of the obtained data suggests that **1** and CO react in the following way (Scheme 2):

Among the products **pphen** and tetracarbonylnickel should be taken out. Their presence is explained by Scheme 3.

According to Scheme 2, the reaction of complex **1** and carbon monoxide involves reduction of nickel(II) to nickel(0) and formation of the dicarbonyl complex together with the profound transformation of the ligand, specifically, the ring aromatization and migration of the double bond within the propenyl substituent.

Attempts to separate **2** and **pphen** using crystallization from different solutions failed. The crystalline adduct, prepared according to Scheme 2, was divided into complex **2** and **pphen** only chromatographically. The isolated individual complex **2** was subjected to crystallization from different solvents (pentane, diethyl ether, toluene, THF, and mixtures). Unfortunately, complex **2** always precipitated as an X-ray amorphous bright red powder.

When **1** reacted with CO under isobaric conditions in a non-flow reactor (P = 1 kg/cm^2, 20 °C), the initial bright green color of the solution quickly turned bright red. The absorption of the gas ceased when the molar ratio of CO:Ni reached 3. From the obtained solution a powdery bright red X-ray amorphous product was prepared with the yield of 90–92%. Its spectra were identical to those of complex **2**. Using GC–MS it was also established that the reaction of

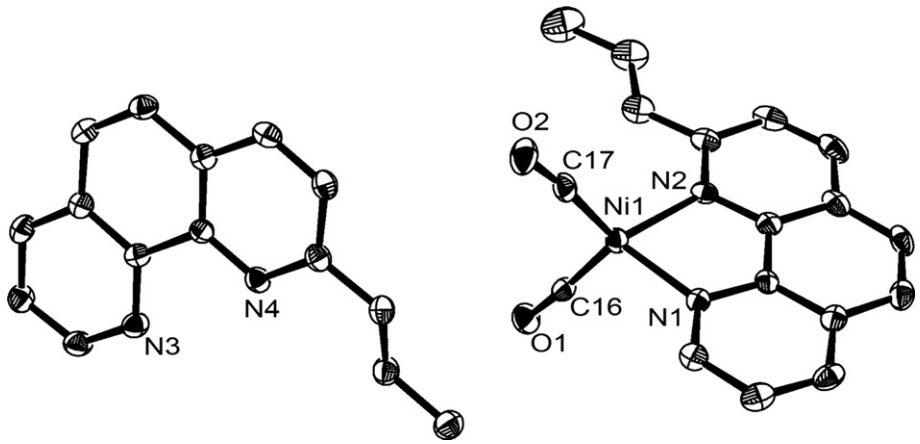

Fig. 1. Molecular structure of adduct of **2** and **pphen**. (ORTEP plot with hydrogen atoms omitted); distances between selected atoms [Å] and angles [°]: Ni–N1 = 2.015(2), Ni–N2 = 2.052(2), Ni–C16 = 1.747(3), Ni–C17 = 1.760(3), C16–O1 = 1.160(4), C17–O2 = 1.151(4), N1–Ni–N2 = 81.47(10), N1–Ni–C16 = 114.42 (12), N2–Ni–C17 = 118.11(12), N2–Ni–C16 = 113.12(12), N1–Ni–C17 = 112.10(12), C16–Ni–C17 = 113.76(14).

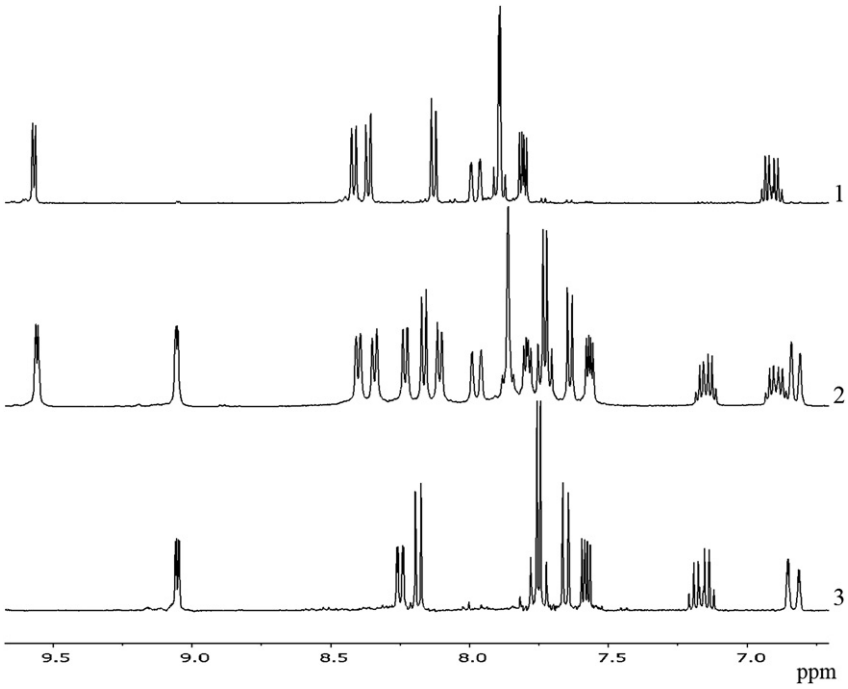

Fig. 2. Informative region of the ^{1}H NMR spectrum for complex **2** (1), solution of crystalline adduct of **2** with **pphen** (2), and free **pphen** (3), 500 MHz, THF-D_8, 297 K.

1 and CO gives rise to acrylic aldehyde in the amount equimolar to the nickel. The detailed analysis of ^{1}H NMR spectra of the reaction solution revealed that in the isobaric system under the used conditions complex **2** forms together with free **pphen**, but, unlike the flow system, in a small amount. The molar ratio of **2**:**pphen** is 1:0.03 according to the integration of quantitative ^{1}H NMR spectra.

The presence of free **pphen** can be explained only by the reversible reaction between **2** and CO (Scheme 3):

The equilibrium constant K_{eq} is 9×10^{-4} for the experiment conditions (P = 1 kg/cm^2, 20 °C); the concentration of CO is assumed to be stationary for the isobaric process. For the reaction in a flow reactor at 20 °C, provided blowing-out of the volatile $Ni(CO)_4$, the equilibrium corresponds to the molar ratio of **2**:**pphen** = 1:1.02 (from the integration of ^{1}H NMR spectra).

The ^{13}C NMR spectrum of complex **2** demonstrates the signal at 197 ppm which is characteristic for carbon monoxide coordinated to nickel [22]. The proton spectrum directs attention to a doublet of doublets widely displaced to low field (9.6 ppm) that indicates to a strong deshielding in the non-substituted aromatic ring of the ligand. For free **pphen** the signal of the analogous proton is located in a higher field at 9 ppm (Table 1).

According to the X-ray structural analysis, the Ni–N bond lengths in complex **2** are significantly longer than those for complex **1** (Ni–N1 = 2.015 Å and 1.921 Å, Ni–N2 2.052 Å and 1.896 Å for **2** and **1** [20], respectively). It is quite consistent with the transformation of the Ni–N δ-bond of **1** to the coordination bond of **2**. The ^{1}H–^{15}N-HMBC spectra of complex **2** have δ^{15}N1 and δ^{15}N2 at −112 and −117 ppm, respectively, whereas in the case of complex **1** δ^{15}N1 = −145. For N2 the ^{1}H–^{15}N-HMBC spectrum contained no cross-peaks that is obviously associated with broadening of the line due to the Ni–N δ-bond. For free **pphen** δ^{15}N1 = −65 and δ^{15}N2 = −76ppm. Thus, the analysis of all the ^{1}H–^{15}N-HMBC data suggests that the nitrogen nuclear in allyl complex **1** is most shielded. It seems to be caused by the essential displacement of electron density to the nitrogen from the metal and allyl group.

The nature of this effect can be better appreciated from an analysis of the proton spectrum of the allyl group in complex **1**.

The ^{1}H NMR spectrum of complex **1** contains signals which differ significantly from the signals reported in the literature for nickel and palladium allyl complexes [23]. First, in contrast with $Ni(allyl)_2$ [23], there is an essential displacement of the signals of the central and anti-protons to low field (Table 1) that is indicative of a substantial deshielding of the protons. At the same time the signals of syn-protons are widely displaced to high field in comparison with those of $Ni(allyl)_2$. There is a significant nonequivalence of both the syn- and anti-protons of the allyl group.

For complex **1** the spin–spin coupling constant for the syn-protons H16s and H18s is 2.1 Hz. This nonequivalence seems to be associated with a strong interaction of the allyl group and imine–amide ligand. The presence of the selective cross-peaks for the protons H16s–H1 and H18s–H10 in the NOESY spectrum (Fig. 3) validates this assumption.

Thus, the interaction with so different in their nature moieties of the imine–amide ligand results in an essential anisotropy in the allyl fragment of the complex. A similar pattern was reported for

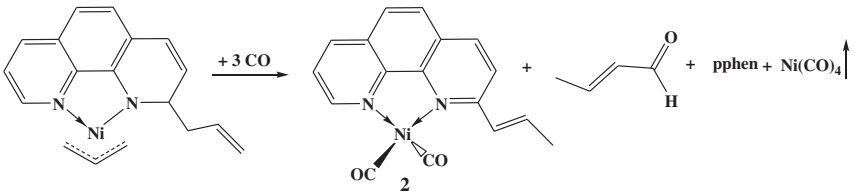

Scheme 2.

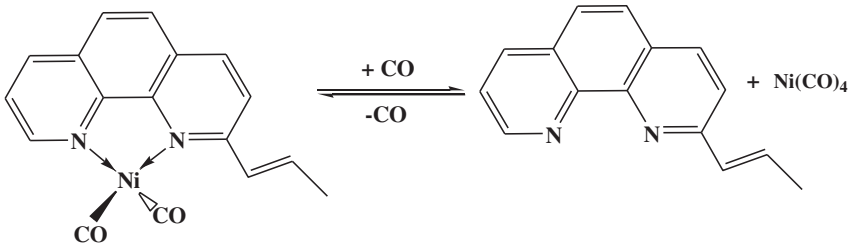

Scheme 3.

the palladium allyl complexes with bulky branched nitrogen-containing ligands [10]. In solution complex **1** exists as an almost equimolar mixture of its *cis*- and *trans*-isomers [20]. The NMR spectra of the *cis*- and *trans*-isomers have no essential differences other than a displacement of the signals that allows clear identification of the isomers. From our viewpoint all the considerations on the spectral data are valid for the both isomers.

The presence of the NOESY selective cross-peaks for the protons of allyl group and imine–amide ligand suggests a significant conjugation of the whole electron system of the nickel ligand surroundings. This is also favorable to the stability of complex **1** despite the formal 16-electron environment.

The vibration spectrum of complex **2** contains two absorption bands at 1970 cm^{-1} and 1875 cm^{-1} characteristic for the carbonyl stretching frequencies ν_{CO} [24]. Similar bands of the carbonyl stretching frequencies are present in the IR spectrum of the nickel dicarbolyl phenanthroline complex Ni(phen)$(CO)_2$ (ν_{CO} = 1980, 1915 cm^{-1}) [25]. The lower values of the carbonyl stretching frequencies for complex **2** in comparison with those for Ni(phen)$(CO)_2$ are indicative of a more limited transition d(Ni)→ π*(CO) and, correspondingly, a more limited total resulting electron donor function of **pphen** as compared to phenanthroline.

The UV/vis spectra of complex **1** (Fig. 4) have bands at 219, 233 nm, and a split one within 268–277 nm which belong to the π→π* transitions in the ligand nitrogen-containing rings. The splitting in the 268–277 nm region seems to be brought about by the nonequivalence of the nitrogen-containing rings one of which is not aromatic but involved in the collective π-conjugation through the double bond. For comparison it should be mentioned that in the considered spectral region phenanthroline has two non-split bands at 221 and 272 nm [26].

Two weak bands at 424 and 454 nm are characteristic for the d-transitions in plane d^8-nickel complexes [27].

For complex **2** the UV/vis spectra demonstrate π→π* bands in almost the same locations (219, 233 and 279 nm), however, it should be mentioned that the long-wave band is not split. It is obviously related to the restoration of the aromaticity of the N-containing ring. Also notice that there are no bands in the d-transition region that is characteristic for the d^{10}-nickel. In [28] a similar effect was reported for the nickel bipyridyl complexes when nickel(II) was reduced to nickel(0). Weak bands within 340–355 nm are attributable to the n→π* transitions of the nitrogen-containing rings [29]. Compared to the similar band of phenanthroline (350–360 nm), the spectrum of complex **2** demonstrates an insignificant blue displacement together with splitting. The blue displacement can be explained by a decrease in the energy of the n-orbital due to the π-p conjugation of the nitrogen electron pair with the allyl group π-system that is quite consistent with the data of the $^1H-^{15}N$-HMBC spectra. The splitting of the band can be connected with a nonequivalence of the electron environment of the nitrogen atoms, in particular, with the influence of the propenyl substituent.

The summation of the spectral data allows us to conclude that the imine–amide ligand in complex **1** has the resulting character of a distinct electron-acceptor. It is well known that the introduction of acceptor ligands in allyl complexes dramatically enhances their stability [8]. Thus, when the imine character of the metal–nitrogen bond transforms to the amide type, the stability of allyl structures in organometallic complexes goes up dramatically that may be responsible for deactivation of catalysts, if this rearrangement takes place during the catalytic cycle. When a further π-acceptor ligand, e.g. carbon monoxide, is introduced at the nickel center, the allyl-nickel group is activated that can lead to the transformation of the imine–amide ligand to the diimine type.

3. Conclusions

The obtained results are rationalized in the form of a scheme representing all the studied transformations (Scheme 4):

The first step of the interaction between the allyl complex and phenanthroline is most likely to be the formation of intermediate labile bis-π–σ allyl complex **a**. Its coordination sphere undergoes a rearrangement which can be regarded as the insertion of the C=N fragment, activated by the coordination to the nickel, into the metal–carbon bond. This reaction results in formation of stable imine–amide complex **1** containing allyl group firmly stabilized in

Table 1
Chemical shifts δ(ppm) for selected atoms[a] of the discussed compounds.

Compound	$\delta_{H16anti}$	$\delta_{H18anti}$	δ_{H17}	δ_{H16syn}	δ_{H18syn}	δ_{H1}	δ_{H10}	δ_{N1}	δ_{N2}
1	*cis*: 2.57 J_{16a-17} = 13.1 *trans*: 2.51 J_{16a-17} = 13.0	*cis*: 2.14 J_{18a-17} = 12.7 *trans*: 2.24 J_{18a-17} = 12.9	*cis*: 5.67 *trans*: 5.87	*cis*: 3.08 J_{16s-17} = 7.0 $J_{16s-18s}$ = 2.1 *trans*: 3.1 J_{16s-17} = 7.0 $J_{16s-18s}$ = 2.2	*cis*: 2.78 J_{18s-17} = 7.4 $J_{18s-16s}$ = 2.1 *trans*: 2.89 J_{18s-17} = 6.9 $J_{18s-16s}$ = 2.0	*cis*: 8.30 *trans*: 8.30	*cis*: 4.32 *trans*: 8.42	−145	–
Ni(allyl)$_2$ [8]	1.67 J_{16a-17} = 14.3		4.9	3.76 J_{16s-17} = 7.6					
2	–	–	–	–	–	9.58	–	−112	−117
pphen	–	–	–	–	–	9.06	–	−65	−77

[a] Atom numbering is in agreement with the molecular fragment at Fig. 3.

the π-form. The coordination of carbon monoxide to **1** most likely brings about the π–σ rearrangement resulting in activation of the allyl group in intermediate complex **b**. Further the coordinated CO inserts into the metal–carbon bond with following β-proton transfer to form a stable heteroaromatic cycle. The process is accompanied by the isomerization of the propenyl substituent leaving the double bond in conjugation with the aromatic ring (intermediate complexes **c** and **d**). The reductive elimination followed by coordination of CO affords the stable diimine complex **2**. Further carbonylation of complex **2** proceeds as a conventional ligand replacement leaving the diimine ligand unchanged.

We concede that the actual mechanism may differ from our proposal in a few details. It is important that our findings indicate the possibility of a profound transformation of nitrogen-containing heterocyclic ligands within the coordination sphere of nickel allyl complexes. For heteroaromatic nitrogen-containing rings such a ready transition from the imine systems to amide ones and back has not been reported in the literature. Our data extend the range of views about the ligand behavior at different steps of the catalyst formation and functioning. In particular, they bring us closer to the understanding why catalysts with diimine ligands (Brookhart's catalysts) have higher stability if hydrogen atoms at the carbon, directly bonded to the nitrogen, are replaced by less labile substituents.

4. Experimental section

4.1. General procedures and materials

Standard vacuum techniques were used in manipulations of volatile and air-sensitive materials.

Infrared spectra were measured for specimens pressed in KBr tablets under argon on an Infralum FT-801 FT spectrometer. Mass spectra were obtained on a Varian MAT spectrometer.

NMR spectra were obtained from on a Bruker AVANCE 500 and an AVANCE II 600 spectrometer. Assignment of ^{1}H, ^{13}C and ^{15}N signals was supported by APT, DEPT-135, COSY, NOESY, TOCSY, HMQC, HSQC and HMBC spectra. Melting points were measured in capillaries sealed under argon and are uncorrected. All NMR experiments were carried out in evacuated and sealed NMR ampoules.

The elemental analysis of the complexes was performed on an FLACH 1112 analyzer (EA series). Nickel content in samples was determined by atomic absorption spectrophotometry on a Carl Zeiss Jena AAS-1 spectrometer using addition method.

UV/vis spectra were recorded with NICOLET spectrometer using all-soldered quartz cuvettes.

Crystal Structure Analysis. Selected crystals were kept under paraffin oil for protection against humidity. For single crystal data collection the crystals were placed in premounted Cryoloops from Hampton Research and cooled down to 100 K, covered with a protecting oil film. Data collection was performed using an Xcalibur diffractometer from Oxford Diffraction, equipped with the Enhance source option and Sapphire CCD detector in φ and ω-scan mode, respectively. The structure was solved by direct methods using SHELXS und refined using SHELXL-97. H atoms were added at idealized positions.

The $Ni(allyl)_2$ complex was prepared according to [8a]. Phenanthroline-1,10 and all the used solvents were purchased (Merck).

Complex **1** was prepared according to [20].

IR: 1463($\delta_a CH_2$, s), 1124 ($\nu_s CCC$, s), 511 (δCCC, s), 291(Ni–N, s) cm^{-1}.

NMR data

cis-isomer: ^{1}H NMR (500 MHz, THF-D_8, 297 K): δ = 8.30 (m, 1H, CH1), 7.14 (dd, $^{3}J_{H2-H1}$ = 13 Hz, $^{3}J_{H2-H3}$ = 8 Hz, 1H, CH2), 7.94 (dd, $^{3}J_{H3-H2}$ = 8.26 Hz, $^{4}J_{H3-H1}$ = 1 Hz, 1H, CH3), 6.76 (dd, $^{3}J_{H5-H6}$ = 7.80 Hz, $^{4}J_{H5-H3}$ = 3.50 Hz, 1H, CH5), 6.25 (dd, $^{3}J_{H6-H5}$ = 8 Hz, $^{4}J_{H6-H8}$ = 3.20 Hz, 1H, CH6), 6.26 (d, $^{3}J_{H8-H9}$ = 9.60 Hz, 1H, CH8), 5.28 (dd, $^{3}J_{H9-H8}$ = 9.57 Hz, $^{3}J_{H9-H10}$ = 4.90 Hz, 1H, CH9), 4.32 (dt, $^{3}J_{H10-H9}$ = 8.10 Hz, $^{3}J_{H10-H13}$ = 4 Hz, 1H, CH10), 2.58 (m, 1H, $CH_2$13), 2.34 (m, 1H, $CH_2$13′), 5.98 (m, 1H, CH14), 5.03 (dm, $^{3}J_{H15trans-H14}$ = 17.2 Hz, $^{2}J_{H15trans-H15cis}$ = 2.2 Hz, 1H, $CH_2$15*trans*), 4.97(dm, $^{3}J_{H15cis-H14}$ = 13.4 Hz, $^{2}J_{H15cis-H15trans}$ = 2.2 Hz, 1H, $CH_2$15*cis*), 3.08 (dd, $^{3}J_{H16syn-H17}$ = 7.0 Hz, $^{4}J_{H16syn-H18syn}$ = 2.10 Hz, 1H, $CH_2$16syn), 2.57 (d, $^{3}J_{H16anti-H17}$ = 13.10 Hz, 1H, $CH_2$16anti), 5.67 (m, 1H, CH17), 2.78 (dd, $^{3}J_{H18syn-H17}$ = 7.40 Hz, $^{4}J_{H18syn-H16syn}$ = 2.04 Hz, 1H, $CH_2$18syn), 2.14 (d, $^{3}J_{H18anti-H17}$ = 12.70 Hz, 1H, $CH_2$18anti) ppm (Fig. 5).

^{13}C NMR (125 MHz, THF-D_8, 297 K): δ = 148.93 (d, $^{1}J_{CH}$ = 180.6 Hz, C1), 121.51 (d, $^{1}J_{CH}$ = 157.74 Hz, C2), 138.22 (d, $^{1}J_{CH}$ = 161.26Hz, C3), 130.93 (s, C4), 128.31 (d, $^{1}J_{CH}$ = 157.75 Hz, C5), 105.22 (d, $^{1}J_{CH}$ = 168.22 Hz, C6), 116.67 (s, C7), 125.65 (d, $^{1}J_{CH}$ = 157.74 Hz, C8), 123.57 (d, $^{1}J_{CH}$ = 158.9 Hz, C9), 63.06 (C10), 155.77 (s, C11), 143.58 (s, C12), 49.56 (C13), 136.17 (C14), 116.04 (t, $^{1}J_{CH}$ = 154.26 Hz, C15), 55.28 (C16), 109.95 (d, $^{1}J_{CH}$ = 159.9 Hz, C17), 48.42 (C18) ppm (Fig. 4).

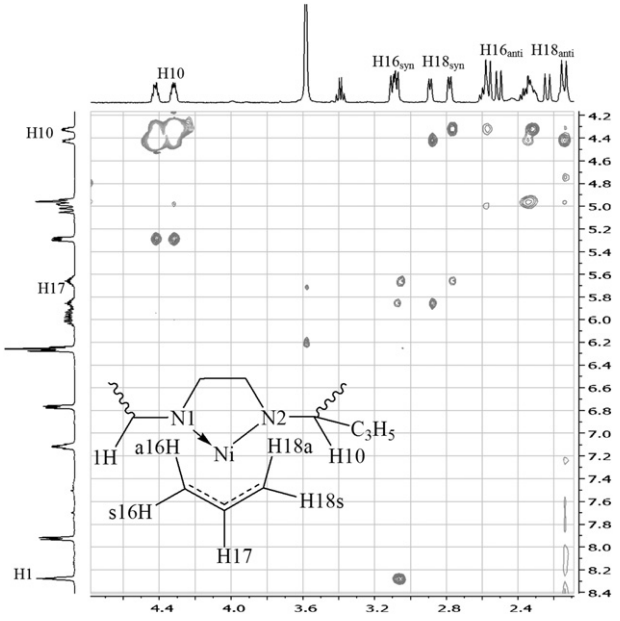

Fig. 3. NOESY spectrum of **1** (*cis*-and *trans*-isomers, details in Experimental section and Supplementary material). Expansion of the region of the allyl group protons of the complexes, 500 MHz, THF-D_8, 297 K.

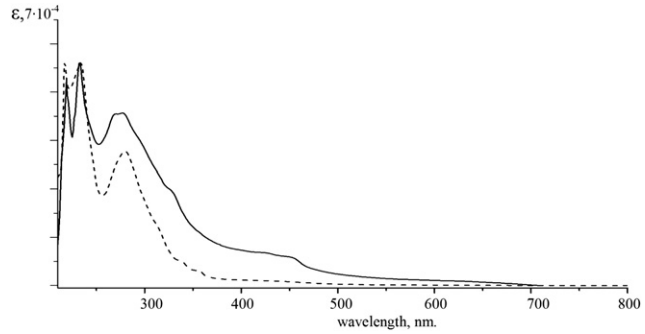

Fig. 4. Absorption UV/vis spectra of **1** (dotted line) and of **2** (solid line).

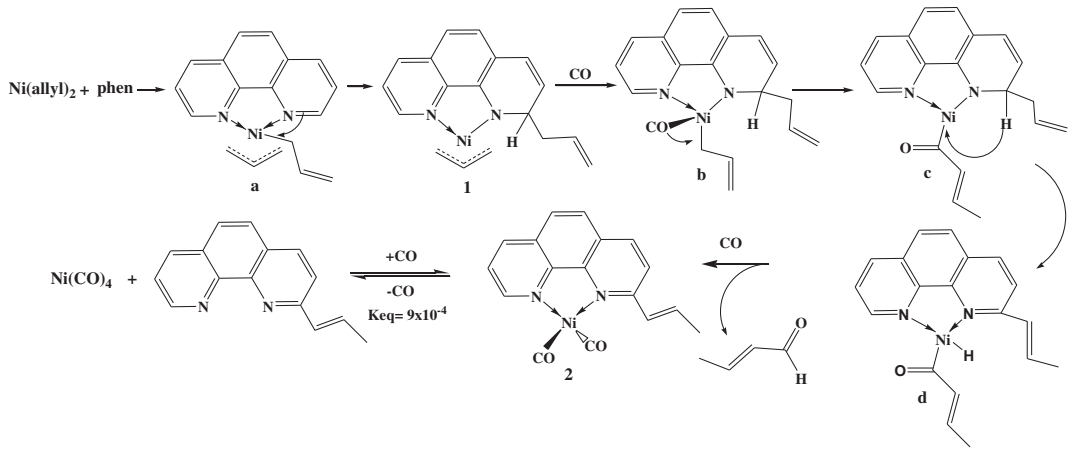

Scheme 4.

^{1}H–^{15}N-HMBC (^{1}H-500 MHz, ^{15}N-50.7 MHz THF-D$_8$, 297 K): $\delta = -145$ (N1), 8.3 (CH1) ppm (Fig. 5).

trans-Isomer: ^{1}H NMR (500 MHz, THF-D$_8$, 297 K): $\delta = 8.30$ (m, 1H, CH1), 7.13 (dd, $^3J_{H2-H1} = 13$ Hz, $^3J_{H2-H3} = 7.55$ Hz, 1H, CH2), 7.94 (dd, $^3J_{H3-H2} = 8.26$ Hz, $^4J_{H3-H1} = 1.0$ Hz, 1H, CH3), 6.765 (dd, $^3J_{H5-H6} = 7.60$ Hz, $^4J_{H5-H3} = 3.40$ Hz, 1H, CH5), 6.25 (dd, $^3J_{H6-H5} = 8$ Hz, $^4J_{H6-H8} = 3.30$ Hz, 1H, CH6), 6.26 (d, $^3J_{H8-H9} = 9.60$ Hz, 1H, CH8), 5.285 (dd, $^3J_{H9-H8} = 9.70$ Hz, $^3J_{H9-H10} = 4.82$ Hz, 1H, CH9), 4.42 (dt, $^3J_{H10-H9} = 7.50$ Hz, $^3J_{H10-H13} = 4.70$ Hz, 1H, CH10), 2.34 (m, 1H, CH13), 2.15 (m, 1H, CH13′), 5.97 (m, 1H, CH14), 4.96 (dm, $^3J_{H15trans-H14} = 10.1$ Hz, $^2J_{H15trans-H15cis} = 2.1$ Hz, 1H, $CH_2$15trans), 4.94 (dm, $^3J_{H15trans-H14} = 8.25$ Hz, 1H, $CH_2$15trans), 3.10 (dd, $^3J_{H16syn-H17} = 7.0$ Hz, $^4J_{H16syn-H18syn} = 2.16$ Hz, 1H, $CH_2$16syn), 2.51 (d, $^3J_{H16anti-H17} = 13.0$ Hz, 1H, $CH_2$16anti), 5.87 (m, 1H, CH17), 2.89 (dd, $^3J_{H18syn-H17} = 6.9$ Hz, $^4J_{H18syn-H16syn} = 2.03$ Hz, 1H, $CH_2$18syn), 2.24 (d, $^3J_{H18anti-H17} = 12.90$ Hz, 1H, $CH_2$18anti) ppm (Fig. 5).

^{13}C NMR (125 MHz, THF-D$_8$, 297 K): $\delta = 149.04$ (d, $^1J_{CH} = 190.42$ Hz, C1), 121.55 (d, $^1J_{CH} = 172.04$ Hz, C2), 138.25 (d, $^1J_{CH} = 150.2$Hz, C3), 131.06 (s, C4), 128.27 (d, $^1J_{CH} = 148.58$ Hz, C5), 105.04 (d, $^1J_{CH} = 168.22$ Hz, C6), 116.90 (s, C7), 125.87 (d, $^1J_{CH} = 156.7$ Hz, C8), 123.59 (d, $^1J_{CH} = 159.3$ Hz, C9), 62.82 (C10), 155.78 (s, C11), 143.84 (s, C12), 48.89 (C13), 136.04 (C14), 115.86 (t, $^1J_{CH} = 153.22$ Hz, C15), 54.9 (C16), 112.65 (d, $^1J_{CH} = 160.16$ Hz, C17), 51.32 (C18) ppm (Fig. 4).

^{1}H–^{15}N-HMBC (^{1}H-500 MHz, ^{15}N-50.7 MHz THF-D$_8$, 297 K): $\delta = -145$ (N1), 8.3 (CH1) ppm (Fig. 5).

4.2. Synthesis of crystalline adduct of *2* and *pphen*

In a flow reactor carbon monoxide was bubbled through a solution of **1** (1.6 g, 5 mmol) in 80 ml of diethyl ether (20 °C, atmospheric pressure, 30 ml/min) until the gas absorption was over. During the initial 15–20 min the starting bright green solution of **1** was turning bright red that was accompanied by the active gas absorption (about 300 ml). Further CO was kept bubbled with the rate of 10 ml/min for 14 h. After that about 80% of the solvent were evaporated under reduced pressure and 5 ml of pentane were added. The resulted solution was kept at −10 °C in a refrigerator for two days and nights. The precipitated crimson-colored crystals were filtered off at −30 °C followed by washing with cold pentane (2 × 10 ml, −30 °C) and vacuum drying for 6 h at 20–25 °C ($P = 10^{-2}$ mmHg). The obtained powdery product is stable in argon and decomposes readily in air with formation of smoke. Yield 0.97 g, 70%.

The crystals begin to decompose with gas evolution at 80–83 °C.

$C_{32}H_{26}N_4NiO_2$ (557.3): calc. C 68.97, H 4.70, N 10.05, Ni 10.53; found C 67.84, H 4.48, N 9.86, Ni 10.42.

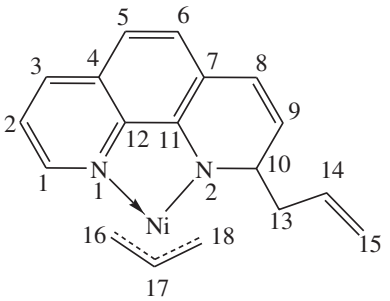

Fig. 5. Numbering scheme of atoms in **1**.

4.3. Synthesis of *2*

a) Crystalline adduct of **2** and **pphen** (0.90 g) was dissolved in 5 ml of diethyl ether-hexane (1:1 v/v). The prepared solution was subjected to the separation with preparative column chromatography (aluminum oxide, height 4 cm, d 25 mm). Red complex **2** was retained in the upper layer of the sorbent and washed with eluent (ether-hexane) to remove **pphen**. Then the red layer was quantitatively carried to a Schlenk flask and extracted with ether (5 × 20 ml) with vigorous shaking. The extracts were combined and about 80% of the initial volume of the solution were evaporated under reduced pressure followed by the addition of 5 ml of pentane and cooling to −30 °C. After 2–3 days a bright red powder precipitated. It was filtered off at −30 °C and dried in vacuum ($P = 10^{-2}$ mmHg) at 20–25 °C for 3 h. Yield 0.16 g, 30%.

b) A solution of complex **1** (1.6 g, 5 mmol) in 80 ml of diethyl ether was vigorously stirred in carbon monoxide atmosphere at 20 °C in a non-flow reactor. The pressure of CO (1 kg/cm^2) was kept constant. During the initial 5 min the starting bright green solution of **1** was turning bright red that was accompanied by the active gas absorption (about 300 ml). After that the reaction was finished, about 80% of the solvent were evaporated under reduced pressure and 5 ml of pentane were added. The resulted solution was kept at −30 °C in a refrigerator. The precipitated crimson-colored crystals were filtered off at −30 °C followed by washing with cold pentane (2 × 10 ml, −30 °C) and vacuum drying for 3 h at 20–25 °C ($P = 10^{-2}$ mmHg). Yield 1.4 g, 85%.

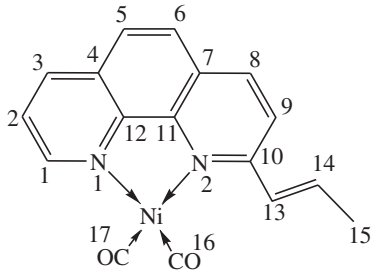

Fig. 6. Numbering scheme of atoms in **2**.

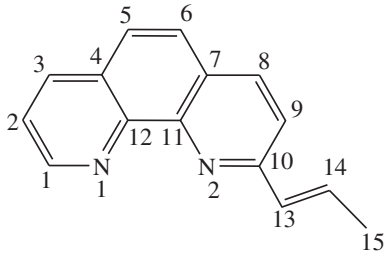

Fig. 7. Numbering scheme of atoms in **pphen**.

The obtained complex **2** is stable in argon and decomposes readily in air with formation of smoke.

Decomp. 60–65 °C. $C_{17}H_{14}N_2NiO_2$ (336.9): calc. C 60.59, H 4.19, N 8.31, Ni 17.42; found C 59.80, H 4.25, N 7.96, Ni 17.36.

MS (70 eV): *m*/*z* (%) = 28(43.0), 41(6.9), 59(11.8), 149(6.3), 181(100.0), 219(30.9), 279(3.2).

IR (KBr) cm^{-1}: 3416(vs), 3042(m), 2963(s), $\nu_{CO(sym)}$1969(s), $\nu_{CO(asym)}$1886(s), 1261(s), 1090(w), 1020(w), 800(s).

^1H NMR (600 MHz, THF-D_8, 297 K): δ = 9.58 (dd, $^3J_{H1-H2}$ = 4.90 Hz, $^4J_{H1-H3}$ = 1.36 Hz, 1H, CH1), 7.81 (dd, $^3J_{H2-H3}$ = 8.03 Hz, $^3J_{H2-H1}$ = 4.86Hz, 1H, CH2), 8.42 (dd, $^3J_{H3-H2}$ = 8.08 Hz, $^4J_{H3-H1}$ = 1.35 Hz, 1H, CH3), 7.90 (d, $^3J_{H5-H6}$ = 8.85 Hz, 1H, CH5), 7.88 (d, $^3J_{H6-H5}$ = 8.85 Hz, 1H, CH6), 8.37 (d, $^3J_{H8-H9}$ = 8.47 Hz, 1H, CH8), 8.14 (d, $^3J_{H9-H8}$ = 8.5 Hz, 1H, CH9), 7.98 (dk, $^3J_{H13-H14}$ = 16.20 Hz, $^4J_{H13-H15}$ = 1.60 Hz, 1H, CH13), 6.92 (dk, $^3J_{H14-H13}$ = 16.30 Hz, $^3J_{H14-H15}$ = 6.80 Hz 1H, CH14), 2.12 (dd, $^3J_{H15-H14}$ = 6.79 Hz, $^4J_{H15-H13}$ = 1.76 Hz, 3H, $CH_3$15) ppm (Fig. 6).

^{13}C NMR (150 MHz, THF-D_8, 297 K): δ = 152.49 (d, $^1J_{CH}$ = 183.56 Hz, C1), 124.80 (d, $^1J_{CH}$ = 167.58Hz, C2), 134.84 (d, $^1J_{CH}$ = 165.88 Hz, C3), 130.66 (s, C4), 126.51 (d, $^1J_{CH}$ = 163.48 Hz, C5), 127.27 (d, $^1J_{CH}$ = 162.46 Hz, C6), 129.06 (s, C7), 135.30 (d, $^1J_{CH}$ = 165.18 Hz, C8), 120.84 (d, $^1J_{CH}$ = 164.84 Hz, C9), 157.38 (s, C10), 145.08 (s, C11), 145.45 (s, C12), 135.10 (d, $^1J_{C13-H13}$ = 160.16 Hz, C13), 134.37 (dk, $^1J_{C14-H14}$ = 151.93 Hz, $^2J_{C14-3H15}$ = 7.78 Hz, C14), 19.30 (dk, $^1J_{C15-3H15}$ = 127.66 Hz, $^2J_{C15-H14}$ = 7.28 Hz, C15), 196.87 (s, C16, C17) ppm (Fig. 6).

$^1H-^{15}N$-HMBC (^1H-500 MHz, ^{15}N-50.7 MHz THF-D_8, 297 K): δ = −112 (N1), 9.58 (H1); −117 (N2), 8.14 (H9) ppm (Fig. 6).

4.4. Synthesis of ***pphen***

Crystalline adduct of **2** and **pphen** (0.90 g) was dissolved in 5 ml of diethyl ether–hexane (1:1 v/v). The prepared solution was subjected to the separation with preparative column chromatography (aluminum oxide, height 4 cm, d 25 mm). Red complex **2** was retained in the upper part of the aluminum oxide column. The eluent (ether–hexane) failed to wash it away, whereas the eluate contained **pphen**. Vacuum evaporation of the eluate gave a light yellow powder which was further recrystallized from heptane. Yield 0.32 g, 90%.

^1H NMR (500 MHz, THF-D_8, 297 K): δ = 9.06 (dd, $^3J_{H1-H2}$ = 4.30Hz, $^4J_{H1-H3}$ = 1.76 Hz, 1H, CH1), 7.58 (dd, $^3J_{H2-H3}$ = 8.10 Hz, $^3J_{H2-H1}$ = 4.27 Hz, 1H, CH2), 8.25 (dd, $^3J_{H3-H2}$ = 8.10 Hz, $^4J_{H3-H1}$ = 1.75 Hz, 1H, CH3), 7.75 (d, $^3J_{H5-H6}$ = 8.80 Hz, 1H, CH5), 7.76 (d, $^3J_{H6-H5}$ = 8.80 Hz, 1H, CH6), 8.19 (d, $^3J_{H8-H9}$ = 8.30 Hz, 1H, CH8), 7.66 (d, $^3J_{H9-H8}$ = 8.30 Hz, 1H, CH9), 6.84 (dk, $^3J_{H13-H14}$ = 15.50 Hz, $^4J_{H13-H15}$ = 1.72 Hz, 1H, CH13), 7.17 (dk, $^3J_{H14-H13}$ = 15.50 Hz, $^3J_{H14-H15}$ = 6.82 Hz 1H, CH14), 2.0 (dd, $^3J_{H15-H14}$ = 6.77 Hz, $^4J_{H15-H13}$ = 1.75 Hz, 3H, $CH_3$15) ppm (Fig. 7).

^{13}C NMR (150 MHz, THF-D_8, 297 K): δ = 150.46 (C1), 123.44 (C2), 136.34 (C3), 129.98 (C4), 126.45 (C5), 127.17 (C6), 128.30 (C7), 136.71 (C8), 121.13 (C9), 156.83 (C10), 147.30 (C11), 147.73 (C12), 133.52 (C13), 132.66 (C14), 18.68 (C15) ppm (Fig. 6).

$^1H-^{15}N$-HMBC (^1H-500 MHz, ^{15}N-50.7 MHz THF-D_8, 297 K): δ = −65 (N1), 9.06 (H1); −77 (N2), 6.84 (H13) ppm (Fig. 7).

Acknowledgements

This work was supported by the Federal Target Program "Research and Training Specialists in Innovative Russia, 2009–2013", (The contract # 14.740.11.0619 for 05.10. 2010). We thank **Vsevolod Sorokin** for the development and making of exclusive glass equipment for the experiments.

Appendix A. Supplementary material

CCDC 774489 contains the supplementary crystallographic data for this paper. These data can be obtained free of charge from The Cambridge Crystallographic Data Centre via www.ccdc.cam.ac.uk/data_request/cif.

Appendix. Supplementary material

Supplementary data associated with this article can be found, in the online version, at doi:10.1016/j.jorganchem.2011.07.022. These data include MOL files and InChIKeys of the most important compounds described in this article.

References

[1] L.K. Johnson, C.M. Killian, M. Brookhart, J. Am. Chem. Soc. 117 (1995) 6414–6415.
[2] Johnson, L.K.; Bennett, M.A.; Ittel, S.D.; Wang, L.; Parthasarathy, A.; Hauptman, E.; Simpson, R.D.; Feldman, J.; Coughlin, E.B. DuPont, WO98/30609 (1998).
[3] S.D. Ittel, L.K. Johnson, M. Brookhart, Chem. Rev. 100 (2000) 1169–1203.
[4] Z. Guan, C.S. Popeney, Top. Organomet. Chem. 26 (2009) 179–220.
[5] (a) F. Blank, C. Janiak, Coord. Chem. Rev. 253 (2009) 827–861;
(b) Y. Yang, P. Yang, C. Zhang, G. Li, X.-J. Yang, B. Wu, C. Janiak, J. Mol. Cat. A: Chem. 296 (2008) 9–17.
[6] H.-Y. Wang, X. Meng, G.-X. Jin, Dalton Trans. (2006) 2579–2585.
[7] L. Li, P.T. Gomes, M.A.N.D.A. Lemos, F. Lemos, Z. Fan, Macromol. Chem. Phys. 212 (2011) 367–374.
[8] (a) G. Wilke, B. Bogdanović, Angew. Chem. 73 (1961) 756;
(b) G. Wilke, B. Bogdanović, P. Hardt, P. Heimbach, W. Keim, M. Kröner, W. Oberkirch, K. Tanaka, E. Steinrücke, D. Walter, H. Zimmermann, Angew. Chem. Int. Ed. Engl. 5 (1966) 151–164;
(c) G. Wilke, Angew. Chem. Int. Ed. 27 (1988) 185–206.
[9] A.R. O'Connor, S.A. Urbin, R.A. Moorhouse, P.S. White, M. Brookhart, Organometallics 28 (2009) 2372–2384.
[10] (a) I. Pairing, A. Moreno, P.S. Pregosin, B. Fuentes, L.F. Veiros, A. Albinati, S. Rizzato, Organometallics 28 (2009) 6489–6506;
(b) S. Filipuzzi, P.S. Pregosin, A. Albinati, S. Rizzato, Organometallics 27 (2008) 437–444.
[11] (a) F. Meyer, H. Kozlowski, Compr. Coord. Chem. 6 (2004) 247–554;
(b) D. Zargarian, Compr. Organomet. Chem. 8 (2007) 133–196.
[12] V.R. Flid, V.B. Kuznetsov, D.V. Dmitriev, Kinet. Catal. 40 (1999) 301–307.

[13] M.D. Leatherman, S.A. Svejda, L.K. Johnson, M. Brookhart, J. Am. Chem. Soc. 125 (2003) 3068–3308.
[14] G. Bai, P. Wei, D.W. Stephan, Organometallics 24 (2005) 5901–5908.
[15] D. Meinhard, P. Reuter, B. Rieger, Organometallics 26 (2007) 751–754.
[16] D.G. Yakhvarov, D.I. Tazeev, O.G. Sinyashin, G. Giambastiani, C. Bianchini, A.M. Segarra, P. Lönnecke, E. Hey-Hawkins, Polyhedron 25 (2006) 1607–1612.
[17] D. Meinhard, M. Wegner, G. Kipiani, A. Hearley, P. Reuter, S. Fischer, O. Marti, B. Rieger, J. Am. Chem. Soc. 129 (2007) 9182–9191.
[18] J. Zhang, H. Gao, Z. Ke, F. Bao, F. Zhu, Q. Wu, J. Mol. Cat. A: Chem. 231 (2005) 27–34.
[19] B. Butschke, H. Schwarz, Organometallics 30 (2011) 1588–1598.
[20] P.B. Kraikivskii, H.-F. Klein, V.V. Saraev, R. Meusinger, I. Svoboda, M. Pashchanka, J. Organomet. Chem. 694 (2009) 3912–3917.
[21] W. Keim, Angew. Chem. 29 (1990) 235–244.
[22] (a) G.M. Bodner, Inor. Chem. 14 (1975);
(b) T. Schaub, U. Radius, Chem. Eur. J. 11 (2005) 5024–5030.
[23] B. Henc, P.W. Jolly, R. Salz, G. Wilke, R. Benn, E.G. Hoffmann, R. Mynott, G. Schroth, K. Seevogel, J.C. Sekutowski, C. Krüger, J. Organomet. Chem 191 (1980) 425–448.
[24] C.A. Tolman, J. Am. Chem. Soc. 92 (1970) 2956–2965.
[25] B.J. Plankey, J.V. Rund, Inorg. Chem. 18 (1979) 957–960.
[26] (a) G.D. Mills, Diss. Abstr. Int. B 33, (1972), in NIST Chemistry WebBook, NIST Standard Reference Database Number 69, Eds.;
(b) P.J. Linstrom, W.G. Mallard, National Institute of Standards and Technology, Gaithersburg MD, 20899, http://webbook.nist.gov, (retrieved March 22, 2011).
[27] A.B.P. Lever, Inorganic Electronic Spectroscopy, second ed. Elsevier, 1984.
[28] A. Klein, A. Kaiser, B. Sarkar, M. Wanner, J. Fiedler, Eur. J. Inorg. Chem. 2007 (2007) 965–976.
[29] D.W. Brown, A.J. Floyd, M. Sainsbury, Organic Spectroscopy. J. Wiley, New York, 1998.